A Robust Decoding Method for OFDM Systems under Multiple Co-channel Narrowband Interferers

Sumit Kumar, Florian Kaltenberger
Eurecom
Biot, France
Email: (sumit.kumar, florian.kaltenberger)@eurecom.fr

Alejandro Ramirez, Bernhard Kloiber
Siemens AG, Corporate Technology
Munich, Germany
Email: (alejandro.ramirez, bernhard.kloiber)@siemens.com

***Abstract*—Software Defined Radio platforms are theoretically capable of operating more than one wireless standard simultaneously. The significant challenges arise when the operating standards use overlapping frequency bands. Co-channel interference (CCI) is one of such challenges which have been in focus of the cellular communication community, but not in the Industrial, Scientific and Medical (ISM) radio bands where multiple heterogeneous wireless standards operate without a centralized coordination. Recognizing Successive Interference Cancellation (SIC) as one of the proven mechanisms to mitigate CCI, we propose methods to improve Packet Error Rate (PER) of wideband OFDM-based systems in the presence of multiple co-channel narrowband interferers. Our methods achieve improvements in PER statistics at lower received power level compared to conventional methods. Reduction in PER of the dominant OFDM signal makes more packets available for regeneration and hence cancellation during SIC procedure which aides the decoding of weaker signal. We also propose a simple yet efficient method to detect the presence and positioning of multiple narrowband interferers. Extensive Monte-Carlo simulations show that our methods elevate a receiver sensitivity gain up to 6 dB and are capable of detecting multiple narrowband interferers simultaneously. Our methods require modifications in the physical layer of the receiver only and hence can be integrated into existing infrastructure.**

I. Introduction

Software defined radios (SDR) have proven their capability of quickly prototyping wireless standards. Some notable examples include gr-IEEE 802.11 [1] for IEEE 802.11g/p, gr-IEEE 802.15.4 for IEEE 802.15.4 [2] and Openairinterface for 4G and 5G[3]. However, application of SDR for reception of the signals conforming heterogeneous wireless standards operating in overlapped frequency bands using the same Radio Frequency (RF) front-end still pose significant challenges from the signal processing perspective [4]. One of such challenges is co-channel interference (CCI), well known and tackled in cellular networks using centralized control over transmit power and transmit time scheduling [5]. This is not the case for Industrial, Scientific and Medical (ISM) bands where heterogeneous wireless standards operate without any centralized control. We denote such networks as *unmanaged networks*. A common example of such network is the 2.4 GHz ISM band crowded by IEEE 802.11g (WiFi), IEEE 802.15.1 (Bluetooth), and IEEE 802.15.4 (ZigBee). All of them suffer significant degradation of throughput even though they possess Carrier Sense Multiple Access with Collision Avoidance (CSMA/CA) ([6],[7],[8]). Major causes include hidden node [9] and differences in channel sensing/response time [10]; an extent of degradation depends on received power levels (RXP) and degree of time/frequency overlap of the signals. In this study, we focus on interference between WiFi and ZigBee in 2.4 GHz band and restrict our comparisons to single antenna systems. Nonetheless, our discussion is applicable to other ISM bands standards and multi-antenna systems without loss of generality. Successive Interference Canceling (SIC) [11] is a proven technique to efficiently mitigate CCI. While SIC primarily found more attention in cellular domain due to centralized co-ordination [5], significant challenges are faced in unmanaged networks. Despite that, several attempts have been made in the past to establish co-existence between WiFi and ZigBee using SIC ([6],[7],[9]). Hidden beneath the disparity of operations of WiFi and ZigBee there lies a favorable condition for SIC which is the operating power level (total power in the entire band) difference of $5-20$ dB between WiFi and ZigBee [10]. This fact is exploited in all the aforementioned state of the art. From the principle of SIC in Fig. 1, it can be observed that efficiency of SIC, in terms of retrieving the weaker signal, depends on how perfectly the stronger signal is regenerated after decoding [5][12]. This, in turn, depends on three factors: RXP of the stronger signal compared to the weaker signal, accuracy of channel estimates of the stronger signal and decoded data of the stronger signal. Methods which facilitate the second and third factors, we term them as *SIC assisting methods*. Some of these methods for unmanaged networks were reported in the past targeting robust channel estimation and better methods of data recovery under interference.

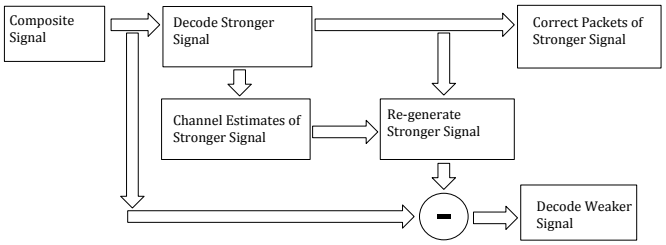

Figure 1: A principle of the Successive Interference Cancellation

In [6], a decision-directed channel estimation along with soft Viterbi decoder for WiFi is used to assist SIC delivering

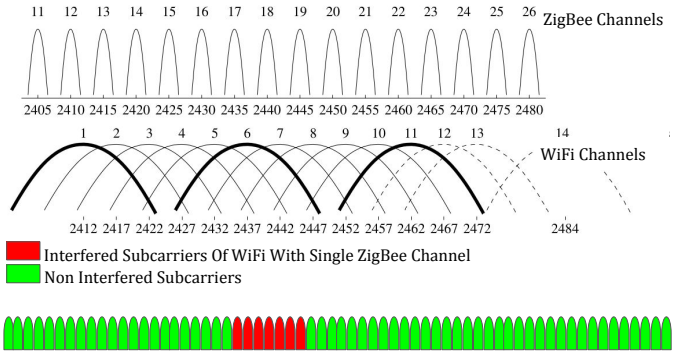

Figure 2: WiFi Subcarriers and Single ZigBee Channel Overlap

a throughput gain for both WiFi and ZigBee. MAC layer enhancements, which benefit from known WiFi preambles are proposed in [7] to assist SIC and increase the throughput of WiFi. However, this method is limited to WiFi-to-WiFi interference and does not address cross-standard interference. In [9], authors propose a data-dependent model of ZigBee to assist SIC along with modifications to the MAC layer to increase the throughput of ZigBee. In [10] and [14], authors propose to send fake preambles and jamming signals to make ZigBee more visible to WiFi and force WiFi to back-off during channel contention. However anti-jamming capabilities of WiFi can make such solutions infeasible [15].

In most of the past works, WiFi is recognized as the culprit for interference and ZigBee as the victim, which is true in majority of the situations, however, in an event of a collision (due to the mismatch in channel sensing and access time), PER of WiFi significantly increases which we discuss in section II. Hence, despite the fact that WiFi is a stronger signal, the performance of SIC in terms of retrieving ZigBee packets degrades because a lesser number of correct WiFi packets are available for regeneration during SIC.

In addition to SIC assisting methods, immediate detection and positioning of interferer (center frequency) is an essential step to be performed before SIC starts. Unfortunately, interference detection and positioning have not been researched widely at the physical layer (PHY) in ISM bands for unmanaged networks. In [16], authors proposed a method to detect ZigBee interference on WiFi by analyzing packet error rate (PER) at the MAC layer. A similar approach was taken by authors of [17] where ZigBee interference to WiFi networks was detected by PER analysis. In [23], authors proposed to detect interference by monitoring soft bit errors in OFDM. However, PER and soft bit error could even occur due to severe fading. Hence, none of the mentioned methods guarantee immediate discovery of the interference. In our work, we have focused on reducing the PER of stronger WiFi signal in an event of collision with multiple narrowband interferers, thereby increasing the number of correct packets of stronger signal during SIC eventually leading towards increased efficiency of SIC.

Our major contributions in this paper are summarized as follows:

- We develop a method to estimate localized noise variances in OFDM-based systems under multiple narrow band interferers and use them to scale the soft bits, i.e., log-likelihood ratios (LLRs) of OFDM subcarriers under interference. A key advantage of our approach is that confidences of LLRs belonging to interfered subcarriers are scaled proportionately giving significant performance gain in terms of PER of WiFi after Viterbi decoding.
- We develop a simple yet effective method to detect the appearance and presence of multiple narrowband interferers. Our method is independent of the individual power levels of interferers and can simultaneously detect multiple low-level interferences.

The remainder of this paper is organized as follows: In Section II we provide details of WiFi and ZigBee interference in the frequency domain. Section III discusses details of our proposed methods. Section IV presents the experimental set-up and concludes with the discussion on results of simulations.

II. WiFi ZigBee Interference: Analysis in Frequency Domain

WiFi is a wideband system with an operating bandwidth of 20 MHz and uses OFDM for PHY in 2.4 GHz band. The entire bandwidth is divided into 64 overlapping, yet orthogonal subcarriers, each 312.5 KHz wide. In contrast, ZigBee operating in 2.4 GHz is a narrowband system with a bandwidth of 2 MHz with and uses O-QPSK (Offset-Quadrature Phase Shift Keying) and DSSS (Direct Sequence Spread Spectrum) for its PHY. Fig. 2 shows within every orthogonal channel (20 MHz each) of WiFi, i.e., $2.412, 2.437, 2.462$ GHz and ZigBee channels (2 MHz each) completely overlap. A magnified view in the frequency domain shown in Fig. 2 reveals an overlap between individual WiFi subcarriers and ZigBee channels. As the bandwidth of each WiFi subcarrier is 312.5 kHz, approximately 7 subcarriers of WiFi are overlapped with each ZigBee channel. We refer to this set of 7 subcarriers as *interfered subcarriers* S_{interf} (plotted in red) and rest of them as *non-interfered subcarriers* $S_{\text{non-interf}}$ (plotted in green). In an event of CCI, noise variance on S_{interf} gets higher than $S_{\text{non-interf}}$ leading to a significant increase of WiFi PER. To get more insight, we performed simulations for a fixed WiFi RXP of -85 dBm under interference from single ZigBee channel RXP varying from -100 dBm to -85 dBm. The PER of WiFi lies in the interval $5-90\%$, while the PER is negligibly small in the absence of interference. This indicates the extent of degradation of the subcarriers corresponding to S_{interf} due to single low power ZigBee channel. Hence, the reliability of LLRs corresponding to S_{interf} needs to be scaled in proportion to the noisiness caused by the interference.

In Section III, we propose the method to estimate noise variance over S_{interf} and $S_{\text{non-interf}}$ locally and apply it to scale the corresponding information.

III. Proposed Methods

A. Local Noise Variance Estimation and LLR scaling

A typical WiFi frame consisting of OFDM data symbols is preceded by preambles known as Short Training Sequence (STS) and Long Training Sequence (LTS) [18]. LTS consists of two identical OFDM symbols which are used for channel estimation. After N (64 for WiFi), point FFT a received WiFi sample in the frequency domain can be written as:

$$Y_{ij} = X_{ij}H_{ij} + n_{ij}, \quad 1 \leq i \leq N, \tag{1}$$

where Y_{ij}, X_{ij} are complex samples representing received and sent symbols on the i-th subcarrier of the j-th OFDM symbol, respectively. Also, in H_{ij} is channel transfer function of the i-th subcarrier for the j-th OFDM symbol. Term n_{ij} contains components from both thermal noise, which is Gaussian and interference, which is not necessarily Gaussian. However, for this work we model both noise sources as Gaussian with zero mean and variance $\sigma^2 = \mathbb{E}\{|n_{ij}|^2\}$. The same LTS is used to compute $\widehat{\sigma}^2$ which is the estimate of actual variance σ^2. The conventional way [19] to obtain $\widehat{\sigma}^2$ is to perform an average over noise variances of all used subcarriers U_{sub} (52 for WiFi [18]) in the LTS as follows:

$$\widehat{\sigma}^2 = \frac{1}{2U_{\text{sub}}} \sum_{i=1}^{U_{\text{sub}}} |Y_{i,1} - Y_{i,2}|^2, \tag{2}$$

where $Y_{i,1}$, $Y_{i,2}$ are the complex samples corresponding to i-th subcarrier of the first and second LTS symbols respectively. $\widehat{\sigma}^2$ is used as noise variance for all U_{sub} of the WiFi OFDM data symbols following the LTS. In a soft decision Viterbi decoder $\widehat{\sigma}^2$ appears as a scaling factor for LLR $\Lambda(y_{ij}^{eq}|s(b_k))$ for every bit b_k. $\Lambda(y_{ij}^{eq}|s(b_k))$ is obtained from i-th equalized subcarrier of j-th OFDM data symbol y_{ij}^{eq} by following a maxlog approximation of maximum likelihood approach over a known subset of alphabets Q_M as mentioned in [22]:

$$\Lambda(y_{ij}^{eq}|s(b_k)) \approx \ln\left(\frac{\max\limits_{s\in Q_M(b_k=0)} \exp\left(-\frac{|y_{ij}^{\text{eq}}-s|^2}{\widehat{\sigma}^2}\right)}{\max\limits_{s\in Q_M(b_k=1)} \exp\left(-\frac{|y_{ij}^{\text{eq}}-s|^2}{\widehat{\sigma}^2}\right)}\right), \tag{3}$$

(3) can be further simplified as:

$$\Lambda(y_{ij}^{eq}|s(b_k)) = \frac{\max\limits_{s\in Q_M(b_k=0)} \left(-|y_{ij}^{\text{eq}}-s|^2\right)}{\widehat{\sigma}^2} - \frac{\max\limits_{s\in Q_M(b_k=1)} \left(-|y_{ij}^{\text{eq}}-s|^2\right)}{\widehat{\sigma}^2} \tag{4}$$

Expression (4) shows that depending on the extent of noise component $\widehat{\sigma}^2$ on the equalized subcarrier y_{ij}^{eq}, $\Lambda(y_{ij}^{eq}|s)$ gets scaled up or down. Expression (4), in case of AWGN, leads to scaling of Λ's corresponding to all y_{ij}^{eq} by the same $\widehat{\sigma}^2$ since $\widehat{\sigma}^2$ does not vary significantly over the subcarriers. This is not the case in the presence of narrowband interference where $\widehat{\sigma}^2$ is higher over S_{interf} compared to $S_{\text{non-interf}}$. Fig. 3 illustrates the difference of noise variances over interfered and non-interfered subcarriers for the case of 4 interferers. In such case, $\widehat{\sigma}^2$ being the average noise variance over entire U_{sub} does not provide local noise variance (LNV)information across the subcarriers. Hence, in the presence of narrowband interferers, local estimation of $\widehat{\sigma}^2$ over S_{interf} and $S_{\text{non-interf}}$ is required in order to justify the scaling of $\Lambda(y_{ij}^{eq}|s)$ as in (4). In our proposed method we separately perform LNV estimation on S_{interf} and $S_{\text{non-interf}}$ and then use them to scale $\Lambda(y_{ij}^{eq}|s)$.

Consider a generalized case of K interferers. S_k is the set of subcarriers affected by the k-th interferer, $k = 1, \ldots, K$ and S_0 is the set of subcarriers unaffected by interference such that $S_0 \cup S_1 \cup S_2 \cup .... \cup S_K = \{1, \ldots, U_{\text{sub}}\}$. For $k = 0, 1, \ldots, K$, the LNV estimate is defined as follows:

$$\widehat{\sigma}^2_{S_k} = \frac{1}{2|S_k|} \sum_{i\in S_k} |Y_{i,1} - Y_{i,2}|^2, \tag{5}$$

and we further define index vector as

$$\left[\boldsymbol{I}_{S_k}\right]_i = \begin{cases} 1, i \in S_k \\ 0, i \notin S_k \end{cases} \qquad i = 1, 2, \ldots, U_{\text{sub}}. \tag{6}$$

Using (5) and (6), the vector of noise variances over U_{sub} is defined as

$$\widehat{\boldsymbol{\sigma}}^2 = \sum_{k=0}^{K} \boldsymbol{I}_{S_k} \widehat{\sigma}^2_{S_k}, \tag{7}$$

Finally using (5), (6) and (7), we can generalize (4) to obtain the scaled LLRs as

$$\Lambda(y_{ij}^{eq}|s(b_k)) = \frac{\max\limits_{s\in Q_M(b_k=0)} \left(-|y_{ij}^{\text{eq}}-s|^2\right)}{\widehat{\sigma_i}^2} - \frac{\max\limits_{s\in Q_M(b_k=1)} \left(-|y_{ij}^{\text{eq}}-s|^2\right)}{\widehat{\sigma_i}^2}, \tag{8}$$

where $\widehat{\sigma_i}^2$ is the i-th element of the vector $\widehat{\boldsymbol{\sigma}}^2$ and $i = 1, 2, \ldots, U_{\text{sub}}$. In Section IV, we scale the LLRs using (8) and examine the PER of WiFi under simultaneous interference from multiple narrowband ZigBee channels.

B. Interference detection with local noise variances

For K number of interferers, the vector of noise variances $\widehat{\boldsymbol{\sigma}}^2$ observes sharp and distinguish rise in magnitude over the regions where noise is higher, i.e., where the narrowband interferers are present compared to the regions unaffected by narrowband interferers. Fig. 3 illustrates the same for the case of 4 ZigBee channels. For a given WiFi channel, the overlapping ZigBee channels center frequencies are known a priori as shown in Fig. 2 and the elevated portions in Fig. 3 give a coarse estimate of the same. We combine this knowledge along with an edge detector in order to pinpoint the interferers as soon as they appear. Our proposed method of interference detection does not add any additional processing complexity since it is a byproduct of our previous method. The key advantage of our approach is that peaks could be obtained even at the very low level of interference. However our method is effective only when there is an overlap between

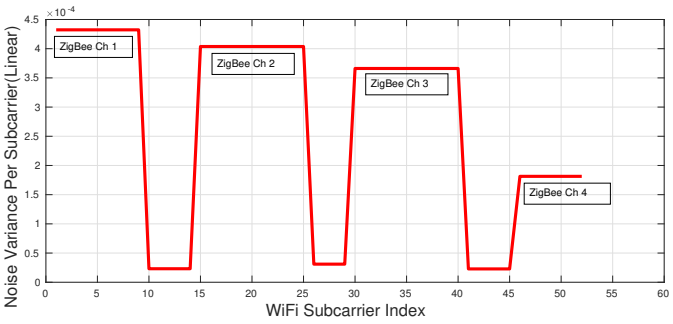

Figure 3: Noise variance per subcarrier for 4 ZigBee interferer

TABLE I: Simulation Parameters

Channel Model	WiFi: 11 tap frequency selective Rayleigh, ZigBee: 1 tap flat fading Rayleigh
Noise Power	-100 dBm
WiFi PSDU	100 bytes
WiFi Modulation and Coding Scheme (MCS)	MCS-0($1/2$ BPSK), MCS-2($1/2$ QPSK), MCS-4($1/2$ 16QAM), MCS-6($2/3$ 64QAM)
ZigBee PSDU	120 bytes
Sampling Rate	WiFi 20 MHz, ZigBee oversampled to 20 MHz
WiFi Simulator	WLAN toolbox, MATLAB Release 2017b
ZigBee Simulator	LRWPAN Class, Communication Systems Toolbox, MATLAB Release 2017b

LTS of WiFi and an ongoing ZigBee transmission as it uses LTS (duration $0.8\,\mu$s) to calculate $\widehat{\sigma}^2$. This is a fair assumption as typical packet lengths of WiFi ($194\,\mu\text{s} - 542\,\mu$s) are shorter than that of ZigBee ($352\,\mu\text{s} - 4256\,\mu$s) [10]. In order to detect the appearance of ZigBee interference during an ongoing WiFi transmission, pilot subcarriers embedded under every OFDM data symbols of WiFi could be used however estimation accuracy could be affected.

IV. Experimental Setup and Results

We perform baseband Monte Carlo simulations using standard compliant 802.11g and 802.15.4 MATLAB packages available in release 2017b of MATLAB to validate our proposed methods. Occasionally, interference between WiFi and ZigBee can lead to WiFi frames undetected, i.e, loss of WiFi frame synchronization [13], but in this work, we assume perfect synchronization of WiFi frames. Additionally, we simulate the worst case scenario ,i.e., there is no CSMA/CA creating 100 % chance of collision. Simulation parameters are mentioned in Table I

A. Local noise variance estimation under multiple interferers and LLR scaling

We simulate interference between single WiFi channel and up to 4 ZigBee channels. RXP of ZigBee channels are fixed to -85 dBm which is the minimum RXP required(in 2.4 GHz band) to achieve 1% PER [20], while WiFi RXP was varied to achieve statistical reliability (in our case, until 300 frames were erroneous). Due to lack of space, we present results for MCS 0, 2, 4, 6. Nonetheless, results follow similar performance curve for other interference RXP and MCS too. We chose WiFi receiver sensitivity as our performance metric for comparison which is the minimum required RXP in order to obtain a PER of 10% [18] without any interference. We compared our method to scale the LLRs as in (8) against the conventional method as in (4). As a reference, we also plot PER of WiFi without interference using the conventional method as in (4) in order to show the extent of PER degradation when multiple interferers appear.

Based on the plots we obtained, as shown in Section IV-A, we observe that with our modifications, 10% PER mark is reached at a lower RXP compared to conventional method for MCS 0, 2, 4, 6. We term the difference in RXP observed between our method and conventional method as *Receiver Sensitivity Gain* which is summarized in Table II.

TABLE II: Receiver Sensitivity Gain(dB)

# of Interferers \ WiFi MCS	0	2	4	6
1	5.4	6.1	5.2	6.5
2	5.8	6.4	5	5.8
4	4	4.7	4.2	5

From Table II we observe that RSG monotonically decreases as the number of interferers increase. Because, as the number of ZigBee channels increase, more WiFi subcarriers get affected which decreases the difference between noise variance estimates calculated using (2) and (5). Additionally, ZigBee power does not decay steeply outside 2 MHz band leading to the addition of noise in more than 7 subcarriers. We also observe that the RSG is consistent throughout the MCS for a given number of interferer. This is due to the fixed payload size of WiFi(100 bytes) which we used for simulations leading to an equal number of LLRs get affected in all the MCS. A direct impact of RSG is that for a given WiFi RXP our method can achieve lesser PER compared to conventional method. This will result in larger number of packets available for regeneration of stronger signal during SIC and hence increasing the performance of SIC.

B. Interference Detection

To test our method of interference detection, we calculate the ratio of the local noise variance (LNV) of the interfered region to that of the region without interference for varying RXP of a single ZigBee channel. We term this ratio as *Noise Level Ratio* (NLR). In the geometrical representation, the level of NLR defines the height of lobes relative to the noise floor as shown in Fig. 3. In Fig. 5, NLR is plotted in log scale while the interference power varies from -100 dBm to -80 dBm. We observe that even at low interference RXP (-100 dBm), the NLR is 6.5 dB which is sufficient to detect the presence of interference.

V. Conclusion

Presence of CCI significantly degrades the receiver's capability to recover a signal. To address this problem, we first introduced a method of fast yet efficient detection of

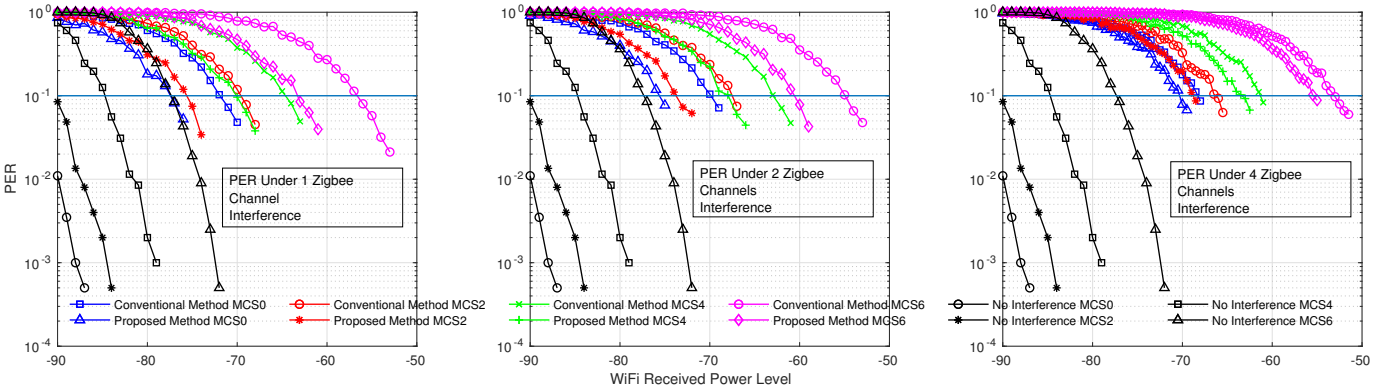

Figure 4: WiFi PER under 1, 2 & 4 ZigBee Interferences

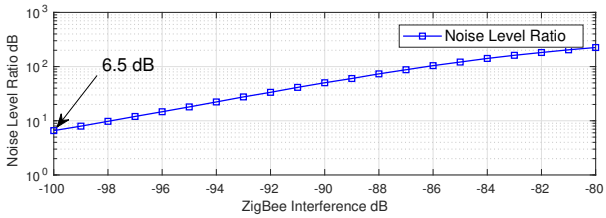

Figure 5: Noise Level Ratio

the presence of multiple narrowband interferers. Secondly, we provided a method to reduce the PER of stronger OFDM signal suffering from multiple narrowband interferers. Our methods thus elevate the robustness of the OFDM-based systems towards narrowband interference as well as aid the performance of SIC during the recovery of weaker narrowband interferers. Although the experimental tests were performed for unmanaged networks, the proposed methods can find potential application in cellular networks too. In future, we extend the system to multi-antenna systems, which will allow increasing the robustness against interference even more by using spatial diversity techniques.

ACKNOWLEDGMENT

This work was supported by Siemens AG, Corporate Technology, Munich and Eurecom, France.

REFERENCES

[1] Bastibl. Bastibl/Gr-ieee802-11. GitHub, Accessed on 1 March . 2018, github.com/bastibl/gr-ieee802-11.
[2] Bastibl. Bastibl/Gr-ieee802-15-4. GitHub, Accessed on 1 March . 2018, github.com/bastibl/gr-ieee802-15-4.
[3] Kaltenberger, Florian, Xiwen Jiang, and Raymond Knopp. "From massive MIMO to C-RAN: the OpenAirInterface 5G testbed."
[4] S. Papadakis, A. Makrogiannakis, M. Surligas and P. Papadakis, "Single SDR multiple primary '&' secondary users emulation platform," 2015 European Conference on Networks and Communications (EuCNC), Paris
[5] Andrews, Jeffrey G. "Interference cancellation for cellular systems: a contemporary overview." IEEE Wireless Communications 12.2 (2005).
[6] Yan, Yubo, et al. "Wizbee: Wise zigbee coexistence via interference cancellation with single antenna." IEEE Transactions on Mobile Computing 14.12 (2015).
[7] Sen, Souvik, et al. "Successive interference cancellation: Carving out mac layer opportunities." IEEE Transactions on Mobile Computing 12.2 (2013).
[8] Azimi-Sadjadi, Babak, et al. "Interference effect on IEEE 802.15. 4 performance." Proceedings of 3rd international conference on networked sensing systems (INNS), Chicago, IL. 2006.
[9] Halperin, Daniel, Thomas Anderson, and David Wetherall. "Taking the sting out of carrier sense: interference cancellation for wireless LANs." Proceedings of the 14th ACM international conference on Mobile computing and networking. ACM, 2008.
[10] Liang, Chieh-Jan Mike, et al. "Surviving wi-fi interference in low power zigbee networks." Proceedings of the 8th ACM Conference on Embedded Networked Sensor Systems. ACM, 2010.
[11] Verdu, Sergio. Multiuser detection. Cambridge university press, 1998.
[12] N. I. Miridakis and D. D. Vergados, "A Survey on the Successive Interference Cancellation Performance for Single-Antenna and Multiple-Antenna OFDM Systems," in IEEE Communications Surveys and Tutorials, vol. 15, no. 1, pp. 312-335.
[13] Yubo, Yan, et al. "Zimo: Building cross-technology mimo to harmonize zigbee smog with wifi flash without intervention." Proceedings of the 19th annual international conference on Mobile computing '&' networking. ACM, 2013.
[14] Zhang, Xinyu, and Kamg G. Shin. "Cooperative carrier signaling: Harmonizing coexisting WPAN and WLAN devices." IEEE/ACM Transactions On Networking 21.2 (2013).
[15] Pelechrinis, Konstantinos, et al. "Ares: an anti-jamming reinforcement system for 802.11 networks." Proceedings of the 5th international conference on Emerging networking experiments and technologies. ACM, 2009.
[16] Croce, Daniele, et al. "Learning from errors: Detecting ZigBee interference in WiFi networks." Ad Hoc Networking Workshop (MED-HOC-NET), 2014 13th Annual Mediterranean. IEEE, 2014.
[17] Croce, Daniele, et al. "Errorsense: Characterizing wifi error patterns for detecting ZigBee interference." Wireless Communications and Mobile Computing Conference (IWCMC), IEEE, 2014.
[18] http://www.ieee802.org/11/
[19] Ren, Guangliang, Huining Zhang, and Yilin Chang. "SNR estimation algorithm based on the preamble for OFDM systems in frequency selective channels." IEEE Transactions on Communications 57.8 (2009).
[20] "http://www.ieee802.org/15/
[21] Tosato, Filippo, and Paola Bisaglia. "Simplified soft-output demapper for binary interleaved COFDM with application to HIPERLAN/2.".ICC 2002.
[22] Robertson, Patrick, Emmanuelle Villebrun, and Peter Hoeher. "A comparison of optimal and sub-optimal MAP decoding algorithms operating in the log domain." Communications, 1995. ICC'95 Seattle.
[23] Gollakota, Shyamnath, et al. "Clearing the RF smog: making 802.11 n robust to cross-technology interference." ACM SIGCOMM Computer Communication Review. Vol. 41. No. 4. ACM, 2011.